

Article

First-Principles Calculations of P-B Co-Doped Cluster N-Type Diamond

Huaqing Lan ¹, Sheng Yang ¹, Wen Yang ¹, Maoyun Di ¹, Hongxing Wang ^{2,*} , Yuming Tian ¹ and Kaiyue Wang ^{1,*} 

¹ School of Materials Science and Engineering, Taiyuan University of Science and Technology, Taiyuan 030024, China

² Key Laboratory of Physical Electronics and Devices, Ministry of Education, School of Electronic Science and Engineering, Xi'an Jiaotong University, Xi'an 710049, China

* Correspondence: hxwangcn@mail.xjtu.edu.cn (H.W.); wangkaiyue@tyust.edu.cn (K.W.)

Abstract: To achieve n-type doping in diamond, extensive investigations employing first principles have been conducted on various models of phosphorus doping and boron–phosphorus co-doping. The primary focus of this study is to comprehensively analyze the formation energy, band structure, density of states, and ionization energy of these structures. It is observed that within a diamond structure solely composed of phosphorus atoms, the formation energy of an individual carbon atom is excessively high. However, the P-V complex substitutes 2 of the 216 carbon atoms, leading to the transformation of diamond from an insulator to a p-type semiconductor. Upon examining the P-B co-doped structure, it is revealed that the doped impurities exhibit a tendency to form more stable cluster configurations. As the separation between the individually doped atoms and the cluster impurity structure increases, the overall stability of the structure diminishes, consequently resulting in an elevation of the ionization energy. Examination of the electronic density of states indicates that the contribution of B atoms to the impurity level is negligible in the case of P-B doping.

Keywords: n-type diamond; donor impurity; phosphorus; cluster formation model



Citation: Lan, H.; Yang, S.; Yang, W.; Di, M.; Wang, H.; Tian, Y.; Wang, K. First-Principles Calculations of P-B Co-Doped Cluster N-Type Diamond. *Crystals* **2024**, *14*, 467. <https://doi.org/10.3390/cryst14050467>

Academic Editor: Vladislav V. Kharton

Received: 28 April 2024

Revised: 12 May 2024

Accepted: 15 May 2024

Published: 16 May 2024



Copyright: © 2024 by the authors. Licensee MDPI, Basel, Switzerland. This article is an open access article distributed under the terms and conditions of the Creative Commons Attribution (CC BY) license (<https://creativecommons.org/licenses/by/4.0/>).

1. Introduction

Given its attractive physical properties, such as ultra-wide forbidden band, high thermal conductivity and high breakdown voltage, diamond is expected to be the ultimate semiconductor for high-power, high-frequency, and high-temperature electronic devices [1–3]. However, since ideal diamond is an insulator, the addition of other elements is necessary to modulate its performance. Doping is one of the most critical processes for electronic devices, and doping diamond with boron allows p-type semiconductors, which can further fabricate some simple p-type devices, such as sensors and agrochemical electrodes [4,5]. But for more complex devices like microprocessors, n-type doping is also necessary for diamond. However, the difficulty in finding a suitable donor makes achieving appropriate n-type doped diamond challenging [6–9].

As a traditional n-type semiconductor impurity, nitrogen (N) has been studied in recent years; Rusevich, L. L has studied the atomic structure and electrical properties of N doping in diamond [10]. In many donors, phosphorus (P) is a promising candidate with a shallow impurity level of only 0.43 eV at the bottom of the conduction band, which is a very excellent donor impurity [11]. Koizumi et al., successfully achieved diamond doping with P atoms in 1997. This proves that P is feasible as a donor impurity. Meanwhile, they also demonstrated that at the P-doped {111} diamond surface, the carrier concentration at 500 K is only $3.8 \times 10^8/\text{cm}^3$, leading to low conductivity [12,13]. Then, the low conductivity of P-doped diamond at room temperature limits its application in the field of electronic devices. To enhance the conductivity of phosphorus-doped diamond, Hu et al., endeavored to introduce boron (B) atoms as compensatory dopants, demonstrating that the conductivity of P-B co-doped diamond surpasses that of P-doped diamond [14]. Recently, the researchers

studied the effect of P as a donor impurity on the N-V (nitrogen-vacancy) center and found that P doping can effectively improve the stability of the NV color center [15]. Zhang et al., used B, P, and S atoms to dope diamond to optimize the activation energy of ions on the surface of the hydrogen-terminated diamond [16].

In addition, it is well known that diamond and related materials have strong quantum vibronic effects, leading to a significant renormalization of the band structure. In 2010, the significant influence of phonon–electron coupling on the temperature-dependent band gap width was discovered [17]. Subsequent studies combining electron–phonon renormalization with molecular dynamics in diamond revealed a more pronounced effect on band width [18]. Kundu et al., suggested inaccuracies in the common methods used to assess electron–phonon coupling in ordered solids [19]. In addition, Yang et al., proposed the utilization of density matrix perturbation theory to evaluate electron–phonon interactions using hybrid functionals for assessing transport properties in light atom-based amorphous semiconductors [20]. In 2024, Kundu et al., explored the impact of quantum vibronic coupling on the electronic characteristics of solid-state spin defects, emphasizing the necessity of integrating quantum vibronic effects into first-principles computations [21]. This paper undertakes a study on diamond P doping and P-B co-doping without the constraints of first-principles density functional theory. The study encompasses various scenarios, including P doping, P-vacancy (V), and the incorporation of two P atoms and one B atom as a doping complex. The analysis focuses on the formation of these complexes in diamond, energy band structures, density of states, and ionization energies.

2. Calculation Method

In this study, the Density Functional Theory-based Sequential Total Energy Package (CASTEP) [22] is employed to optimize the theoretical structure through computational calculations. The interaction potential between ions and valence electrons is modeled using ultra-soft pseudopotentials. Atomic relaxation exchange–correlation energy is characterized by the Perdew–Burke–Ernzerhof (PBE) parameterized expression of the Generalized Gradient Approximation (GGA) [23,24]. A plane-wave basis set was established, and periodic boundary conditions were implemented to ascertain the Kohn–Sham ground state. The system under investigation comprises a periodic supercell containing 216 atoms arranged in a $(3 \times 3 \times 3)$ configuration. The Monkhorst–Pack k-point grid was employed to sample the Brillouin zone in reciprocal space during the self-consistent calculation process to determine the electronic ground state [25]. In the selection of K points, $(2 \times 2 \times 2)$, $(3 \times 3 \times 3)$, $(4 \times 4 \times 4)$, and $(6 \times 6 \times 6)$ were chosen. When selecting the $(2 \times 2 \times 2)$ k point, the energy band structure was too loose and simple; thus, it was difficult to effectively observe the relationship between the impurity level and the conduction band. The results obtained by $(3 \times 3 \times 3)$, $(4 \times 4 \times 4)$, and $(6 \times 6 \times 6)$ were close, while the calculation time used in $(4 \times 4 \times 4)$ and $(6 \times 6 \times 6)$ were several times that of $(3 \times 3 \times 3)$. While constantly adjusting the convergence accuracy and the truncation energy, a higher truncation energy, as well as a smaller convergence criterion, was chosen to improve the computational accuracy as much as possible, and the results showed it was in convergence when the residual force of each atom was less than 5×10^{-4} eV/Å. Therefore, each atomic residual force was selected as less than 10^{-3} eV/Å, and on this basis, the truncation energy was tried from 450 eV to 900 eV, at intervals of 50 eV. The partial P-B co-doping structure at less than 700 eV did not converge, and the result of greater than 800 eV was consistent with 750 eV, but the calculation time was well beyond 750 eV. As such, a grid of k-points with dimensions of $(3 \times 3 \times 3)$ was employed for sampling in convergence test calculations, alongside a fixed energy cutoff of 750 eV across all computational procedures. Geometric optimizations were performed iteratively until the residual forces acting on individual atoms reached a magnitude below 10^{-3} eV/Å.

The ionization energy, band structure calculations, and density of state (DOS) details were obtained with the Heyd–Scuseria–Ernzerhof (HSE) 06 functional [26,27], and the minimum accuracy of convergence at the truncation energy of 750 eV was chosen. The

convergence criterion of the inter-atomic forces was set to be 10^{-3} eV/Å, and the energy of self-consistent calculation was 1.0×10^{-5} eV/atom.

In particular, this study isolated electron pairs in the doping process so that each atom has insufficient or extra eight atoms and so that the calculation of the electron density of band structure causes the formation of four electrons around each atom. This study also selected “use formal spin as initial = 0” during the calculation.

3. Results and Discussion

3.1. Pure Diamond

The band width of pure diamond was calculated using different calculation methods to verify the accuracy of the calculation method, with GGA-PBE, GGA-PW 91, and GGA-WC obtaining less than 4.5 eV, while the band width was up to 12.776 eV by Nlocal-HF function. And the band results obtained from HSE06 and HSE03 calculations for pure diamond, which are 5.381 eV and 5.243 eV, respectively, closely approximate the experimental value of 5.480 eV [28], so the relatively better HSE06 was selected as the calculation method of energy band, density of electron states, and ionization energy.

3.2. P-Doped Diamond

The diamond structure of P and P-V (phosphate-vacancy) doping was found for P and vacancy coordination doping, including P and B as the doping element, as shown in Figure 1.

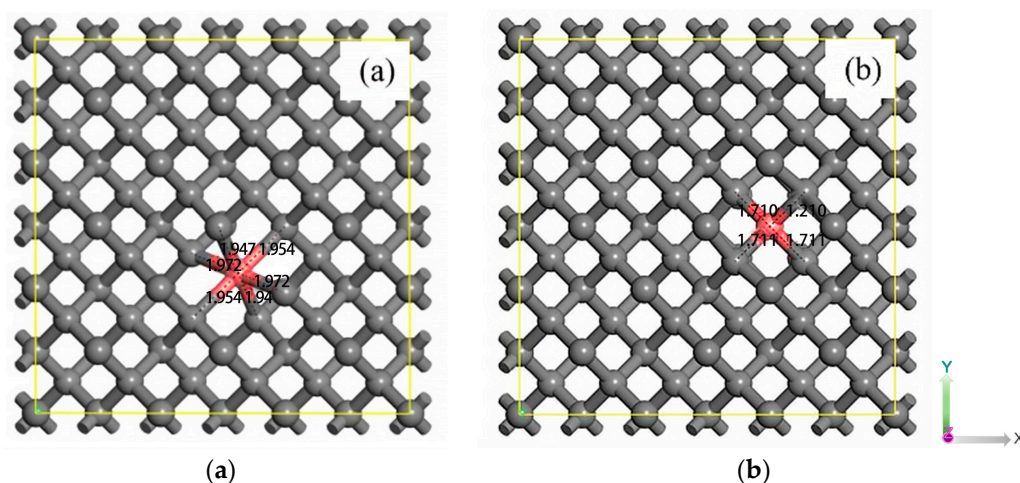


Figure 1. The P-doped diamond model: (a) P-V doping, (b) P doping. The gray is carbon; the pink is phosphorus.

3.2.1. Defect Structures

Figure 1a,b depicts the geometric characterization of the P-V and P-substituted carbon structures within a $3 \times 3 \times 3$ supercell, as well as the carbon structure containing a single P atom, respectively. The optimized structures of these configurations are detailed in Figure 1, revealing covalent bond lengths between phosphorus (P) and carbon (C) atoms in the P-V structure measuring 1.972 Å, 1.947 Å, and 1.954 Å, which closely align with the findings reported by Sichuan Nie et al. [29]. The covalent bonds around the P atoms in the P-doped structure are elongated up to 1.711 Å and 1.710 Å. Table 1 reveals that the average lattice constant of P-V-doped diamond expands by 0.018 Å in comparison to pristine diamond. Conversely, for P-doped diamond, the average lattice constant increases by 0.052 Å, which is 1.8 times greater than that of P-V-doped diamond. The volumes of the three structures were calculated as 1225.1804 Å³, 1231.3734 Å³, and 1243.0787 Å³. Analysis of the lattice volumes indicates that both P-V doping and P doping induce lattice distortions, with the distortion resulting from P doping significantly exceeding that from P-V doping.

Table 1. Bond lengths for P-V doping and P doping.

Structure	Lattice Constant a (Å)	Lattice Constant b (Å)	Lattice Constant c (Å)
C ₂₁₆	10.7004	10.7004	10.7004
C ₂₁₄ P ₁ V ₀	10.7236	10.7131	10.7185
C ₂₁₅ P ₁	10.7636	10.7636	10.7296

3.2.2. Impurity Formation Energy

The formation energy is calculated to investigate the stability and most likely doping impurities. The formation energy of X in charge state q is calculated using the following equation:

$$E_f(X, q) = E_{tot}[X, q] - E_{tot}[bulk] - \sum n_i \mu_i + q[E_F + E_V + \Delta E] \quad (1)$$

In the context of this study, $E_{tot}[X, q]$ represents the total energy of the supercell hosting the impurity X in the charge states state q . The parameter $E_{tot}[bulk]$ corresponds to the total energy of the pristine bulk within an analogous supercell. The variable n_i signifies the count of type i atoms (either host atoms or impurity atoms) introduced ($n_i > 0$) or removed ($n_i < 0$) from the supercell. Additionally, μ_i denotes the chemical potential of the atoms under consideration. The chemical potentials of P and B are computed from hybrid calculations conducted in the gas phase involving P₂H₆ and BH₃. Furthermore, E_F represents the Fermi level, while E_V designates the energy of the valence band maximum of the bulk diamond. The symbol ΔE is utilized as the correction factor necessary to align the electrostatic potentials between the bulk material and the defective supercell [30–32].

In Table 2 the formation energy of C₂₁₅P₁ is 7.493 eV, and the formation energy of C₂₁₄P₁V₀ is 5.702 eV. Compared with Professor Dai's study, the formation energy of P-V doping is 6.18 eV, and the conclusion is close but relatively low [33]. According to the phenomenon in 3.2.1, the lattice distortion caused by P-V doping is less than that of P doping, and the formation energy of P-V doping is relatively small, which indicates that the P-V doping form is more stable in P-doped diamond. However, the formation energy of the single vacancy of 5.790 eV is close to and lower than the formation energy of the P-V structure.

Table 2. Formation energy of the P and P-V diamond.

Structure	Defect	Formation Energy (eV)
C ₂₁₅ P ₁	P	7.493
C ₂₁₄ P ₁ V ₀	P-V	5.702
C ₂₁₅ V ₀	V	5.790

3.2.3. Band Structure and DOS

Figure 1a illustrates the doping structure of P-V, revealing the presence of six C atoms and P atoms with only five outer electrons. This configuration indicates that P atoms in the diamond lattice, as P⁵⁺ ions, substitute C⁴⁺ ions for doping. Consequently, the impurity level and Fermi level are expected to reside at the bottom of the conduction band. P⁵⁺ ions supply five electrons to the diamond lattice, one more than C⁴⁺ ions, thereby functioning as donor impurities upon doping. However, in the P-V complex, P-V⁵⁺ is doped in place of two C⁴⁺ ions, leading to the release of electrons to the lattice structure and the absorption of three electrons. As a result, the complex exhibits characteristics of a dominant impurity.

The electronic properties of P-doped diamond were examined through calculations of the band structure and electronic density of states of P-V complexes, as depicted in Figure 2. Analysis of the doped electronic structure revealed that the impurity and Fermi levels of the P-V complexes are positioned proximate to the upper region of the valence band, with the impurity level situated below the Fermi level. The band structure of P-doped diamond exhibits characteristics akin to a typical n-type semiconductor, where the impurity level and Fermi level align in the vicinity of the conduction band. And in Kundu's study, the

negatively charged nitrogen vacancy center in diamond has an impact on the band due to electron–phonon coupling [21]. Considering that the doping structure of P-V is similar to that of N-V, there may also be an electron–phonon coupling effect in P-V-doped diamond, causing quantum vibration and leading to deviation in the band structure. Nonetheless, the impurity level of P-doped diamond remains insufficiently elevated to breach into the conduction band. This phenomenon may be attributed to the significantly higher doping concentration utilized in the simulation calculations compared to the typical ion injection concentration (3 ppm). Furthermore, the compact nature of the overall structure and the limited number of atoms contribute to the pronounced doping effects observed.

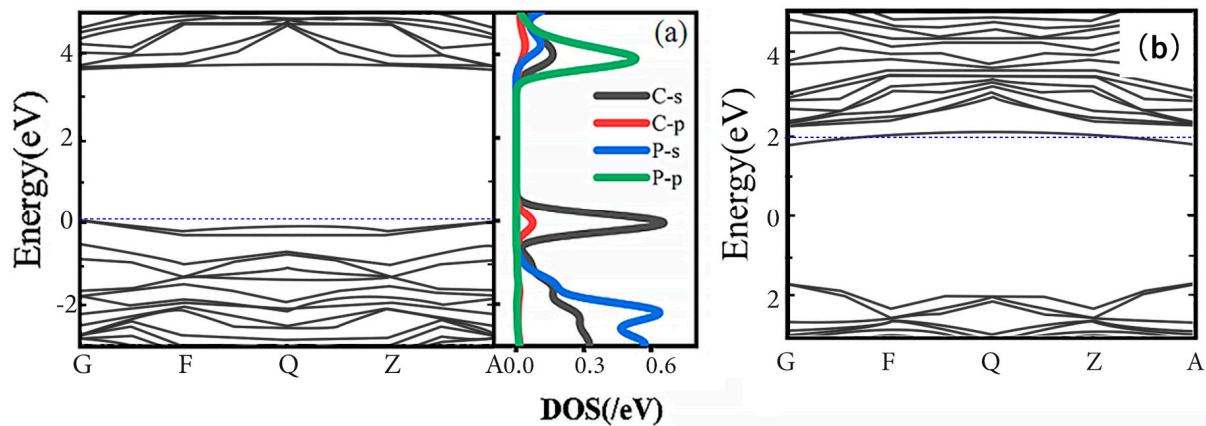


Figure 2. Band and electron density of states: (a) P-V doping (b) P doping. Blue dashed line is the Fermi level.

Upon examining the density of states in P-V doping, it has been discerned that the impurity level predominantly originates from the s orbital of carbon atoms, with a portion also stemming from the p orbital of carbon. The shallow nature of the impurity energy level supplied by the carbon atom precludes it from enhancing carrier mobility as a composite center within the semiconductor framework. While the impurity level in the P-V doping configuration is distinct, featuring minimal structural distortion and a lower binding energy in comparison to the P-doped structure, the band structure analysis reveals that diamond doped with the P-V complex conforms to the archetype of a P-type semiconductor. Nonetheless, the substantial lattice distortion induced by phosphorus doping in diamond, coupled with the relatively elevated formation energy, renders both doping configurations unsuitable for n-type semiconductor applications.

The energy band of the structure has two split impurity levels of approximately 0.7 eV above the valence band, contributed by the s-orbitals of the C. Although the P-V doping structure is more stable than the P substitution doping, the band structure shows that the impurity level of the P substitution doping is located near the conduction band and has a typical n-type semiconductor band feature. However, P-V-doped diamond is a typical P-type semiconductor that is not suitable for applications in n-type devices.

3.3. P-B Co-Doped Diamond

In terms of the conclusion in Section 3.2, it is difficult for phosphorus-doped diamonds to satisfy the requirements of diamonds used as n-type semiconductors. There are two main difficulties:

- (a) The excessive atomic radius of the P atom leads to the distortion of the diamond lattice, thereby compromising the stability of the P-substituted doped structure and subsequently impacting the functionality of phosphorus-doped diamond as an n-type semiconductor.
- (b) The introduction of phosphorus ions into diamond can give rise to P-V doping; however, this configuration consistently exhibits the hallmark traits of predominant

impurities in p-type semiconductors, presenting a contradiction to the objective of developing n-type semiconductors. This inherent characteristic also detrimentally impacts the overall semiconductor performance [34].

To augment the doping concentration of phosphorus in diamond, the inclusion of compensatory elements is a viable strategy. Notably, the incorporation of boron atoms as the principal dopant in diamond has advanced to a proficient level, owing to the comparable atomic radii of boron and carbon atoms. Moreover, the outermost electron shell of boron comprises three electrons, potentially facilitating the generation of holes within the diamond lattice. It is pertinent to highlight that, as per Equation (2) [35], the effective impurity energy concentration in the diamond should be N_D^*

$$N_D^* = N_D - N_A > n_i \quad (2)$$

where N_D^* is the effective donor concentration, N_D is the donor concentration, N_A is the acceptor concentration, and n_i is the intrinsic carrier concentration.

From the structure of N as a cluster state, Dai Ying et al. [15] constructed some P-B co-doped structures containing two P atoms and one B atom as shown in Figure 3. Although the minimum concentration of doping was used in $(3 \times 3 \times 3)$, the doping concentration was as high as 278 ppm. This doping concentration was nearly a hundred times different than the 3 ppm that could be achieved in practice. And to achieve the actual doping concentration, it required the larger model structure, about $(14 \times 14 \times 14)$, so the structure with a small doping concentration could only be selected as far as possible for simulation calculation.

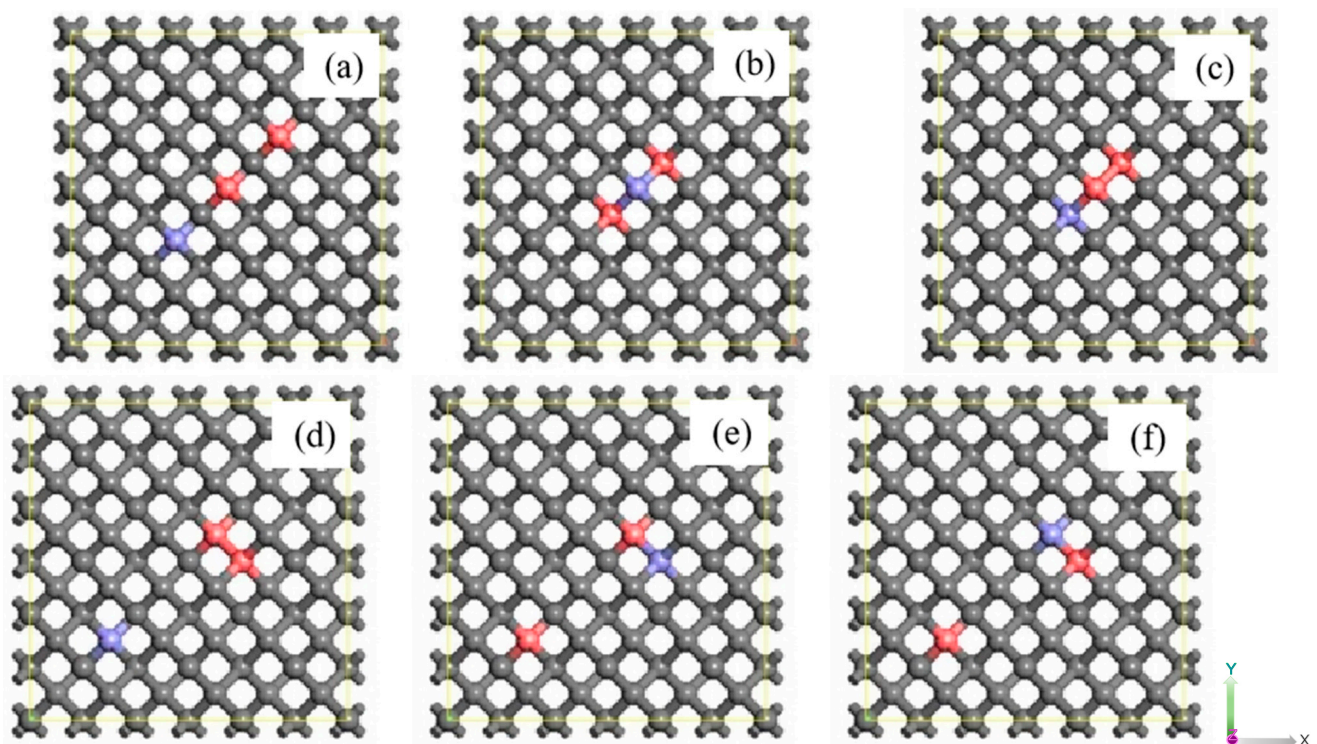


Figure 3. The P-B co-doped diamond structure: (a) P-C-P-C-B, (b) P-B-P, (c) P-P-B, (d) P-P-C-C-C-B, (e) B-P-C-C-C-P, (f) P-B-C-C-C-P. The gray is carbon, the purple is phosphorus, and the pink is boron.

3.3.1. Defect Structures

Figure 3 delineates the comprehensive doping configuration involving two phosphorus atoms and one boron atom, serving as a partially illustrative paradigm of diamond impurities. All configurations undergo structural optimization utilizing the GGA-PBE methodology. The P-B co-doped configuration is segmented into the P-P complex as the cluster state, with B existing as individual atoms, and P-B forming the cluster state structure,

while P represents the fundamental model for the individual atoms. Within Figure 3, model (b) and (c) form the fundamental framework for the two sets of model pairs. Notably, due to non-identical characteristics of the B atoms and the two P atoms, the P atoms situated further from the B atoms are denoted as P1, while those in close proximity to the B atoms are designated as P2. Figure 3d–f lists the doping of different cluster state structures with a cluster state structure and a single atomic doping form, respectively, where the least number of C atoms between the cluster state structure and the individual atoms is the number of C in the structure. For example, in (d), the cluster structure is PP, independent atoms are B, and the minimum number of intermediate C is 3, so the doping structure is written as P-P-C-C-C-B.

The determination of lattice volumes in diamond structures doped with various complexes is conducted independently based on lattice indices. Specifically, in Table 3 the lattice volume of diamond in the P₃ complex is calculated at 1260.5618 Å³, whereas the overall lattice volumes of diamond doped with the P-B complex exhibit relatively smaller values of 1253.5401 Å³, 1252.2964 Å³, and 1252.5516 Å³, respectively. Upon P₃ doping, three P⁵⁺ ions substitute three C⁴⁺ ions and introduce three electrons into the diamond structure. In contrast, the P₃ structure induces significant lattice distortion upon integration into the diamond lattice, while the P-B co-doped scenario only contributes an electron to the diamond structure, yet effectively mitigates lattice distortion.

Table 3. Bond lengths for P-V doping and P doping.

Structure	lattice Constant a (Å)	Lattice Constant b (Å)	Lattice Constant c (Å)
C ₂₁₃ P ₃	10.7950	10.8173	10.7950
C ₂₁₃ P-P-B	10.7834	10.7794	10.7842
C ₂₁₃ P-B-P	10.7741	10.7811	10.7811
C ₂₁₁ P-C-P-C-B	10.7878	10.7753	10.7754

3.3.2. Impurity Formation Energy

The C₂₁₃P-B-P and C₂₁₃P-P-B are calculated from Formula 1 as 9.436 eV, 11.325 eV, respectively. The other doped structure energies are shown in Table 4. The formation energy of these P-B co-doped diamonds is significantly lower than that of C₂₁₃P₃, which fully proves that B can improve the solubility of P atoms in diamond. Among them, P-P-B and P-B-P have lower formation energy than other non-cluster formation models.

Table 4. Formation energy of P-B co-doped types.

Defect	Formation Energy (eV)
P-P-B	10.32
P-C-P-C-B	19.43
P-B-P	13.83
P-P-C-B	15.67
P-P-C-C-B	16.04
P-P-C-C-C-B	16.03
B-P-C-C-C-P	17.34
B-P-C-C-P	17.26
B-P-C-P	16.67
P-P-P	25.35

The formation energy necessary for the incorporation of a P-C-P-C-B complex as an impurity into a diamond lattice surpasses that of alternative P-B co-doped configurations. It is noteworthy that the triad of atoms functioning as cluster states exhibit a diminished formation energy in comparison to the cluster arrangement involving two impurities and an individual atom, collectively contributing to the formation of a doped diamond structure. In contrast to the individual-form doping approach, the cluster configuration induces significant lattice distortions yet entails a lower formation energy, rendering it susceptible

to facilitate formation albeit with inherent structural instability. The induced lattice distortions may exert a substantial influence on the physical properties of diamond.

3.3.3. Band Structure and Dos

Figure 4 displays the four band structures of the doped diamond, illustrating the configurations nearest and farthest from the cluster state structure. Each band structure reveals the distinctive n-type semiconductor characteristics of a P-B co-doped diamond with two P atoms and one B atom. The proximity of the impurity and Fermi levels increases as the distance between the individual atoms and the cluster state diminishes. Ultimately, when the individual atoms and the cluster structure consisting of three atoms align, the impurity level transitions into the conduction band, resembling the band structure of P-doped diamond. This phenomenon may be attributed to the interplay between the distance and coupling of the cluster state structure and individual atoms, influencing the electron behavior of the donor atoms. As the distance decreases, the impact of the cluster state structure and individual atoms on the electron behavior diminishes, resulting in a more pronounced doping effect from the individual atoms. Additionally, the influence of the compensation atoms B is less significant than that of the P atoms in this context.

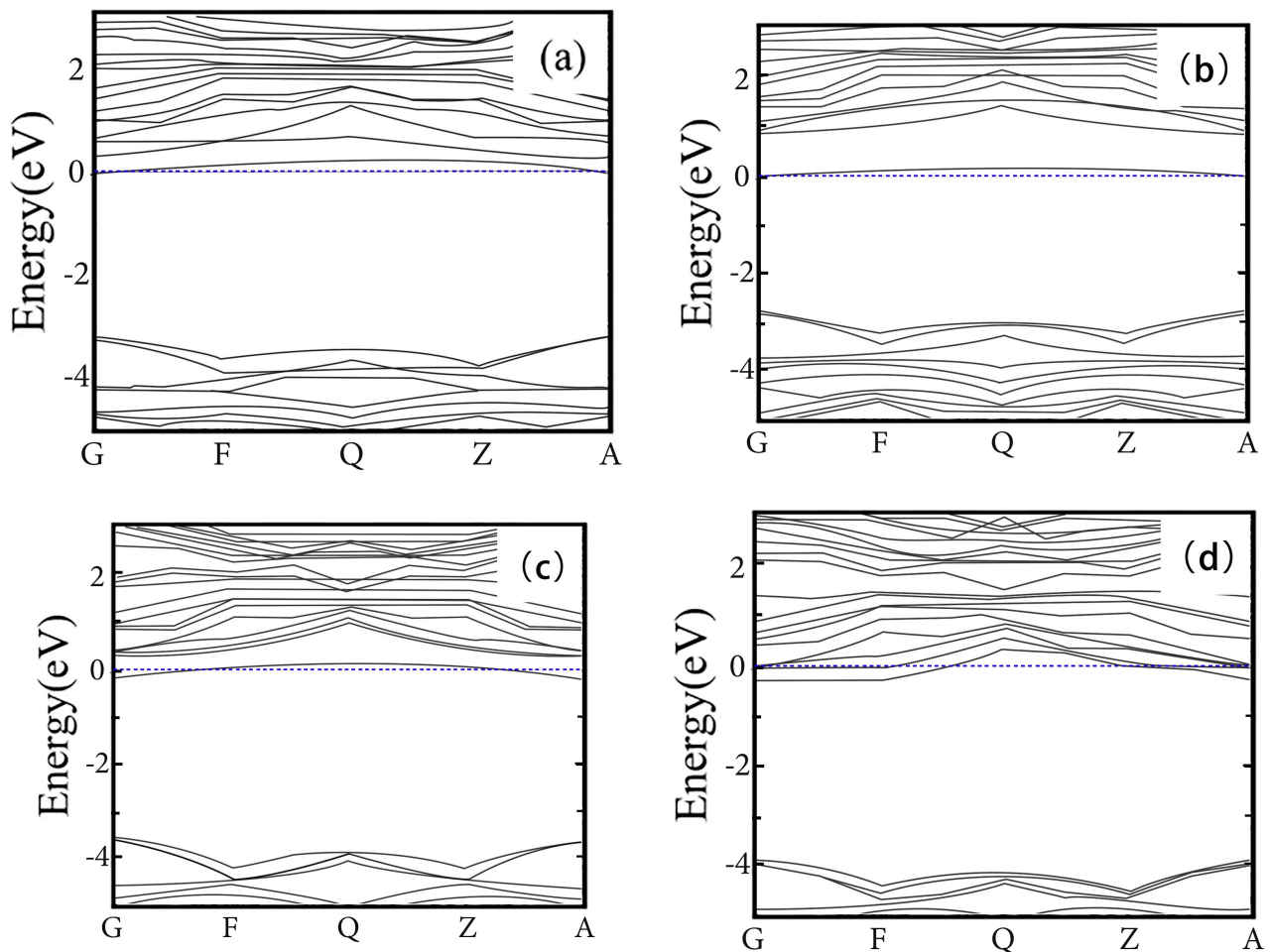


Figure 4. P-B co-doped diamond band structures: (a) P-P-B, (b) P-C-P-C-B, (c) P-P-C-C-C-B, (d) B-P-C-C-C-P. (The blue dotted line is the Fermi energy level).

In Figure 4c,d, a comparison is made between the scenarios where a P-P cluster state structure is employed and B atoms serve as individual impurity atoms. While the distance between the individual B atoms and P ions varies, approaching and receding from the conduction band, the presence of three C atoms between them is consistent.

Upon examining the electron density guided by B ions in Figure 5c, it is evident that the contribution of the individual B atoms to the impurity level is not significant, with the impurity level primarily influenced by the presence of P atoms. This observation highlights the pronounced compensation effect of B atoms on P-doped diamond, indicating that the introduction of the three atoms as a cluster state structure results in the formation of a deep impurity level, which plays a crucial role in semiconductor recombination processes.

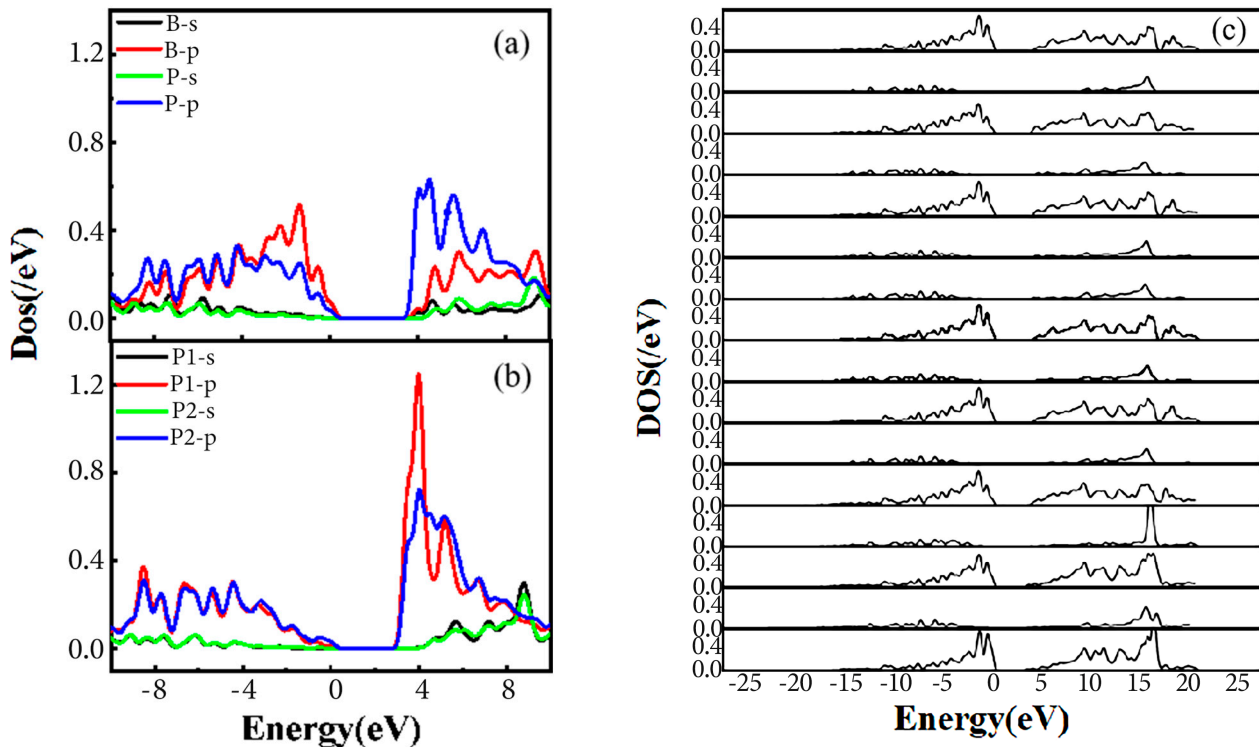


Figure 5. P-B co-doped diamond electron density of states (a,b): Density of state of PBP, PCPCB, (c): Electronic density of states of the B atoms in all structures (PPB, PPCB, PPCCB, PPCCCB, PCPB, PCCPB, PCCCPB, PCBP, PCCBP, PCCCBP, PBP, PCPC).

Figure 5a,b depicts the electronic density of states for two distinct doping configurations: (a) P-B-P and (b) P-C-P-C-B. In the former structure, a representative cluster state arrangement is observed, with two P atoms positioned symmetrically and exhibiting nearly identical electronic density of state profiles. Conversely, in the latter structure, the doped atoms are not in direct proximity, and the two P atoms do not occupy symmetric positions, leading to a lack of direct interaction. A comparison between the electronic density of states of different P atoms in the P-P complex in Figure 6 and the electronic density of states of the B atom in Figure 5c reveals that the B atom, when in contact with the P atom, does not significantly contribute to the impurity level, with all impurity levels primarily originating from the P atom. The s- and p-orbital energy of the forbidden B atoms are below 0.6 eV, while the distant P atoms have energies up to 1.2 eV.

Figure 5c illustrates that the B atoms in all P-B co-doped structures contribute very little to the impurity level, whether through s- or p-orbitals, which exist solely in the valence or conduction band. Hence, it is crucial to analyze the electronic structure of P atoms. In Figure 6, the s-orbital of the P atoms produces negligible hybridization, resulting in minimal contribution to the band. Furthermore, when two P atoms are bonded to different B atoms, one of the P atoms, which is away from the B atoms, is the primary contributor to the donor energy level. As the B atoms approach the P-P cluster state structure, the contribution of the two phosphorus atoms to the donor energy level becomes similar. In Figures 7 and 8, it is shown that when a P atom is bonded to a B atom to form a cluster state structure, the P atoms far away from the P-B cluster state structure contribute significantly to the donor

energy level. Although the electronic density of states of the P atoms in the P-P and P-B clusters are similar, as well as the overall trend, the P atoms far away from the B atoms are the primary contributors to the donor energy level.

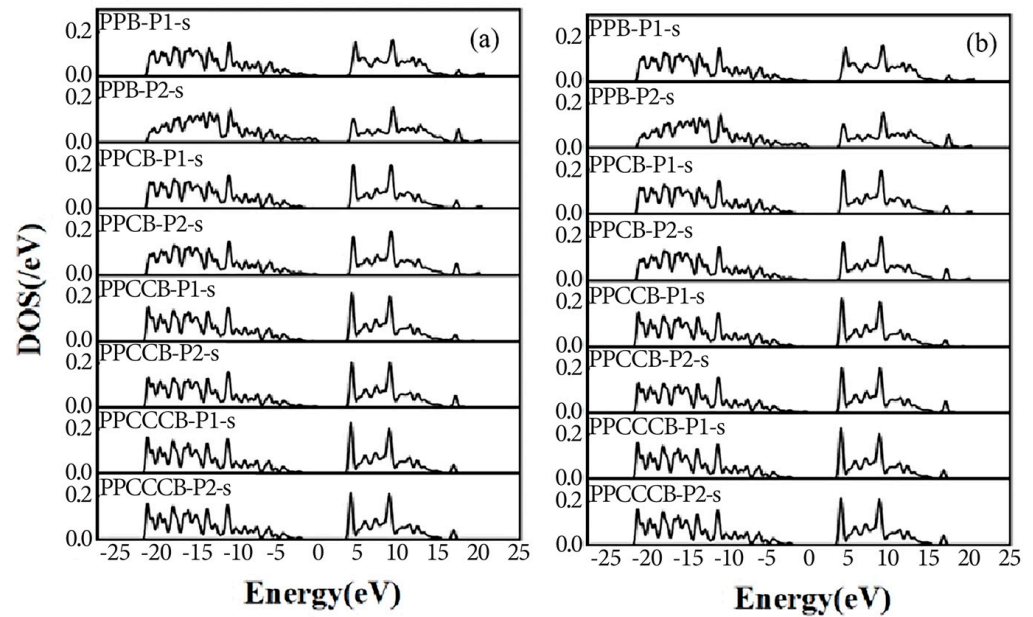


Figure 6. (a) s-orbit of the P-P cluster structure; (b) p-orbit of the P-P cluster structure.

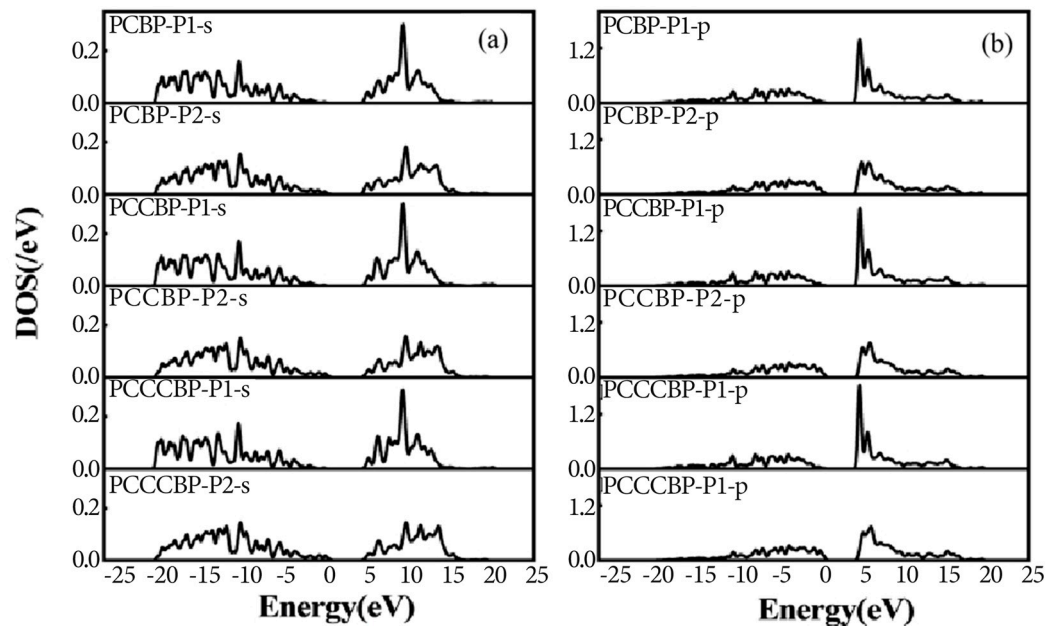


Figure 7. (a) s-orbit of the B-P cluster structure; (b) p-orbit of the B-P cluster structure.

The impurity structures are contrasted in Figures 7a and 8a by comparing a cluster state structure consisting of P atoms and B atoms with an individual P atom doping structure. The density of electronic states in the two configurations is found to be highly similar, with the B atoms having minimal impact on the impurity level when in contact with P atoms. In Figures 6–8, despite the differing distances between B atoms and two P atoms, the proximity of two P atoms to B atoms results in a lower contribution to the impurity level as the distance to B atoms decreases. This observation suggests a significant influence of atom B on atom P, as the electron orbits of the two atoms interact when in close proximity.

The B atoms and nearby P atoms exhibit complementary electron pairing, leading to a lack of contribution to the impurity level in diamond. The change in the band structure with the distance between the doped atoms may be the influence of the electron–phonon coupling effect of the doped atoms.

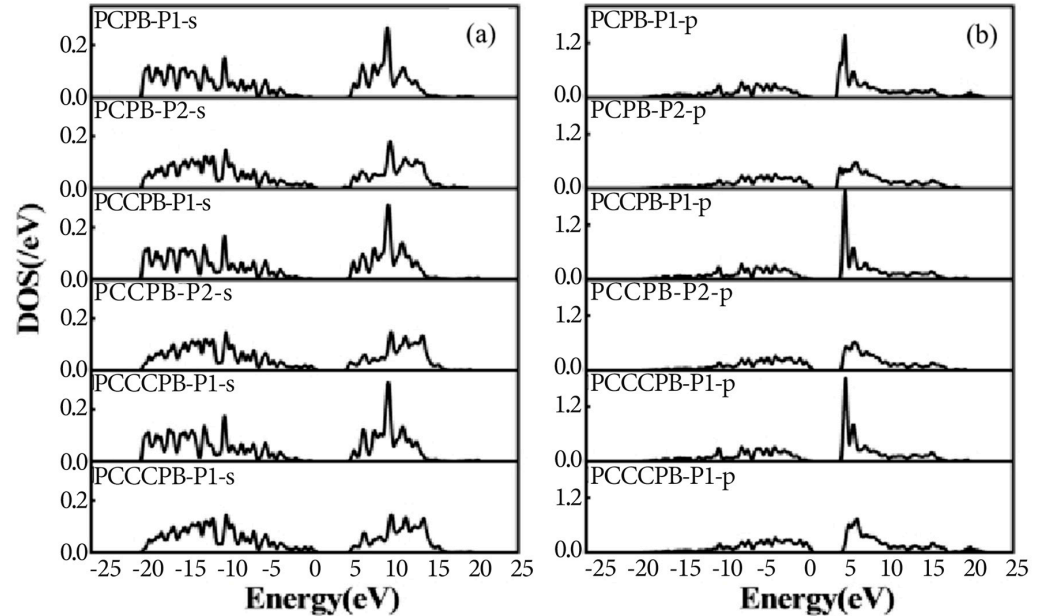


Figure 8. (a) s-orbit of the P-B cluster structure; (b) p-orbit of the P-B cluster structure.

3.3.4. Ionization Energy

The ionization energy associated with the thermodynamic transition level $\epsilon(q_0/q_1)$ is determined through the calculation prescribed by the pertinent equation. In this context, the thermodynamic transition is precisely characterized as the Fermi-level locus at which the formation energies of the charge states q_0 and q_1 attain equilibrium.

$$\epsilon(q_0/q_1) = \frac{E_{tot}[X, q_0] - E_{tot}[X, q_1]}{q_0 - q_1} - (E_v + \Delta V) \quad (3)$$

Here, $E_{tot}[X, q_0]$ represents the total energies of the supercell housing the impurity X in the charge states q_0 , and $E_{tot}[X, q_1]$ represents the total energies of the supercell housing the impurity X in the charge states q_1 , respectively. E_v denotes the energy of the valence band maximum of the bulk diamond. V stands for the correction factor utilized to align the electrostatic potentials between the bulk material and the defective supercell. The donor level $\epsilon(0/+)$ corresponds to the donor ionization (donor level) energy of E_D .

In Table 5, it is observed that the ionization energy of P-P-B and P-B-P structures is notably lower compared to other configurations. Conversely, the P-C-P-C-B structure, with three atoms positioned at a distance from each other, exhibits a relatively high ionization energy. This study demonstrates that the formation of defects in an aggregated state results in decreased energy levels and ionization energies within P-B co-doped diamond. Specifically, a configuration containing a single P atom displays a higher ionization energy in contrast to a configuration with a single B atom. Moreover, as the distance between atoms in the individual atom cluster state structure increases, there is a gradual rise in the required ionization energy. This phenomenon can be attributed to the tightly packed diamond structure, where impurities located within the carbon lattice hinder the escape of electrons bound to carbon atoms. Consequently, doping in a cluster state structure proves to be an effective method to reduce ionization energy and enhance electron mobility to a certain extent.

Table 5. Ionization energies of diamond co-doped with P-P-B, P-B-P, and P-C-P-C-B atoms.

Compound	Ion Energy (eV)
P-P-B	1.68
P-C-P-C-B	2.45
P-B-P	1.52
P-P-C-B	1.73
P-P-C-C-B	1.84
P-P-C-C-C-B	2.12
P-B-C-C-C-P	2.32
P-B-C-C-P	2.13
P-B-C-P	1.91

4. Conclusions

This article investigates the doped configurations involving phosphorus (P) in diamond. Specifically, P atoms infiltrate the diamond lattice solely as impurities, exhibiting a propensity for forming complexes with vacancies. This preference arises from the substantial lattice distortion induced by the substitutional incorporation of P, leading to a significantly higher formation energy compared to the P-vacancy (P-V) configuration. In the P-V-doped diamond, P finds itself encompassed by six neighboring carbon atoms, thereby assuming an electron-receiving state. Such a circumstance contradicts the objective of employing P doping to engineer n-type semiconductors, consequently discouraging the utilization of P-V co-doped.

The introduction of B as a compensatory impurity in diamond can markedly enhance the doping concentration of P atoms and mitigate lattice distortion. In contrast to the P-V configuration, structures incorporating two P atoms and one B atom in co-doped arrangements exhibit shallow donor levels, thereby facilitating the production of individual carriers.

The P-B co-doped structure involves the use of B atoms as auxiliary impurities that enhance the solubility of P atoms, as well as the electronic and band structures. Simultaneously, the distance between P and B atoms significantly affects the formation energy of the electronic density of states' band structure. A greater distance between P and B atoms results in a higher formation energy, and the impurity level is closer to the conduction band. These findings demonstrate that the cluster state structure is more stable and clearer when one B atom is used for doping. There may be deviations in the band changes of all structures under the influence of right electron–phonon coupling.

From the point of view of the electron density of states and the ionization energy, the doping structure with only cluster states during P-B co-doped significantly outperformed the other structures. In summary, in the context of P-B co-doping, the cluster state exhibits favorable electronic properties; however, it also induces significant lattice distortion. Consequently, the size of the cluster state exerts a substantial impact on diamond's behavior as an n-type semiconductor in experimental settings. This observation is important for experimental guidance and can serve as a valuable reference.

Author Contributions: Conceptualization, H.L.; methodology, H.L.; software, W.Y.; validation, H.L.; formal analysis, H.L.; investigation, M.D.; resources, K.W.; data curation, H.L.; writing—original draft preparation, H.L.; writing—review and editing, H.L. and Y.T.; visualization, S.Y.; supervision, K.W. and M.D.; project administration, K.W.; funding acquisition, K.W. and H.W. All authors have read and agreed to the published version of the manuscript.

Funding: This work was supported by National Natural Science Foundation of China [grant number U21A2073] and Shanxi Province Natural Science Foundation [grant number 202203021211210]. The Graduate Education Innovation Program of Taiyuan University of Science and Technology [SY2023004]. The Scientific and Technological Innovation Programs of Higher Education Institutions in Shanxi [2022L304].

Data Availability Statement: The original contributions presented in the study are included in the article, further inquiries can be directed to the corresponding authors.

Acknowledgments: Thanks to Di Maoyun and Yang Wen for their theoretical guidance while writing.

Conflicts of Interest: The authors declare no conflict of interests.

References

1. Collins, A.T.; Davies, G. (Eds.) *Properties and Growth of Diamond*; INSPEC: London, UK, 1994; Chapter 9.7; pp. 261–288.
2. Isberg, J.; Hammersberg, J.; Johansson, E.; Wikstrom, T.; Twitchen, D.J.; Whitehead, A.J.; Coe, S.E.; Scarsbrook, G.A. High carrier mobility in single-crystal plasma-deposited diamond. *Science* **2002**, *297*, 1670–1672. [[CrossRef](#)] [[PubMed](#)]
3. Shen, W.; Shen, S.N.; Liu, S.; Li, H.; Nie, S.Y.; Pan, Y.H.; Tian, Z.; Li, Q. Binding of hydrogen to phosphorus dopant in phosphorus-doped diamond surfaces: A density functional theory study. *Appl. Surf. Sci.* **2019**, *471*, 309–317. [[CrossRef](#)]
4. Nebel, C.E. From gemstone to semiconductor. *Nat. Mater.* **2003**, *2*, 431. [[CrossRef](#)] [[PubMed](#)]
5. Visser, E.P.; Bauhuis, G.J.; Janssen, G.; Vollenberg, W.; Giling, L.J. Electrical conduction in homoepitaxial, boron-doped diamond films. *J. Phys. Condens. Matter* **1999**, *4*, 7365. [[CrossRef](#)]
6. Kato, H.; Yamasaki, S.; Okushi, H. n-type doping of (001)-oriented single-crystalline diamond by phosphorus. *Appl. Phys. Lett.* **2005**, *86*, 1899. [[CrossRef](#)]
7. Zvanut, M.E.; Carlos, W.E.; Freitas, J.A.; Jamison, K.D.; Hellmer, R.P. Identification of phosphorus in diamond thin films using electron paramagnetic-resonance spectroscopy. *Appl. Phys. Lett.* **1994**, *65*, 2287–2289. [[CrossRef](#)]
8. Je, L. Substitutional oxygen-nitrogen pair in diamond—Art. no. 115206. *Phys. Rev. B* **2003**, *67*, 115206.
9. Anderson, A.B.; Mehandru, S.P. n-type dopants and conduction-band electrons in diamond: Cluster molecular-orbital theory. *Phys. Rev. B Condens. Matter* **1993**, *48*, 4423. [[CrossRef](#)] [[PubMed](#)]
10. Rusevich, L.L.; Kotomin, E.A.; Popov, A.I.; Aiello, G.; Scherer, T.A.; Lushchik, A. The vibrational and dielectric properties of diamond with N impurities: First principles study. *Diam. Relat. Mater.* **2022**, *130*, 109399. [[CrossRef](#)]
11. Prins, J.F. Ion-implantation n-type diamond: Electrical evidence. *Diam. Relat. Mater.* **1995**, *4*, 580–585. [[CrossRef](#)]
12. Alexenko, A.E.; Spitsyn, B.V. Semiconducting diamonds made in the USSR. *Diam. Relat. Mater.* **1992**, *1*, 705–709. [[CrossRef](#)]
13. Saito, T.; Kameta, M.; Kusakabe, K.; Morooka, S.; Maeda, H.; Asano, T. Synthesis of phosphorus-doped homoepitaxial diamond by microwave plasma-assisted chemical vapor deposition using triethylphosphine as the dopant. *Diam. Relat. Mater.* **1998**, *7*, 560–564. [[CrossRef](#)]
14. Hu, X.J.; Li, R.B.; Shen, H.S.; Dai, Y.B.; He, X.C. Electrical and structural properties of boron and phosphorus co-doped diamond films. *Carbon* **2004**, *42*, 1501–1506. [[CrossRef](#)]
15. Zou, D.; Shen, S.; Li, L.; Wang, Q.; Liang, K.; Chen, L.; Wu, G.; Shen, W. Influence of phosphorus donor on the NV center in diamond: A first-principles study. *Phys. B Condens. Matter* **2024**, *676*, 415614. [[CrossRef](#)]
16. Zhang, C.; Ma, X.; Qi, Z.; Liu, X.; Ren, Y. The effect of B/P/S doping on Li⁺ charge transfer during ion transport along the H-diamond surface: A first-principles calculation. *Diam. Relat. Mater.* **2023**, *135*, 109846. [[CrossRef](#)]
17. Giustino, F.; Louie, S.G.; Cohen, M.L. Electron-phonon renormalization of the direct band gap of diamond. *Phys. Rev. Lett.* **2010**, *105*, 265501. [[CrossRef](#)] [[PubMed](#)]
18. Kundu, A.; Govoni, M.; Yang, H.; Ceriotti, M.; Gygi, F.; Galli, G. Quantum vibronic effects on the electronic properties of solid and molecular carbon. *Phys. Rev. Mater.* **2021**, *5*, L070801. [[CrossRef](#)]
19. Kundu, A.; Song, Y.; Galli, G. Influence of nuclear quantum effects on the electronic properties of amorphous carbon. *Proc. Natl. Acad. Sci. USA* **2022**, *119*, e2203083119. [[CrossRef](#)] [[PubMed](#)]
20. Yang, H.; Govoni, M.; Kundu, A.; Galli, G. Computational protocol to evaluate electron-phonon interactions within density matrix perturbation theory. *J. Chem. Theory Comput.* **2022**, *18*, 6031–6042. [[CrossRef](#)]
21. Kundu, A.; Galli, G. Quantum Vibronic Effects on the Excitation Energies of the Nitrogen-Vacancy Center in Diamond. *J. Phys. Chem. Lett.* **2024**, *15*, 802–810. [[CrossRef](#)]
22. Clark, J.S.; Segall, D.M.; Pickard, J.C.; Hasnip, P.J.; Probert, M.I.; Refson, K.; Payne, M.C. First principles methods using CASTEP. *Z. Für Krist.* **2005**, *220*, 567–570. [[CrossRef](#)]
23. Perdew, J.P.; Burke, K.; Wang, Y. Generalized gradient approximation for the exchange-correlation hole of a many-electron system. *Phys. Rev. B* **1996**, *54*, 16533–16539. [[CrossRef](#)]
24. Hammer, B.; Hansen, L.B.; Norskov, J.K. Improved adsorption energetics within density-functional theory using revised Perdew-Burke-Ernzerhof functionals. *Phys. Rev. B* **1999**, *59*, 7413–7421. [[CrossRef](#)]
25. Monkhorst, H.J.; Pack, J.D. Special points for Brillouin-zone integrations. *Phys. Rev. B* **1976**, *13*, 5188–5192. [[CrossRef](#)]
26. Heyd, J.; Scuseria, G.E.; Ernzerhof, M. Hybrid functionals based on a screened coulomb466 potential. *J. Chem. Phys.* **2003**, *118*, 8207–8215. [[CrossRef](#)]
27. Heyd, J.; Scuseria, G.E.; Ernzerhof, M. Hybrid functional based on a screened coulomb potential. *J. Chem. Phys.* **2006**, *124*, 219906. [[CrossRef](#)]
28. Czelej, K.; Spiewak, P.; Kurzydowski, K.J. Electronic structure and n-type doping in diamond from first principles. *MRS Adv.* **2016**, *1*, 1093–1098. [[CrossRef](#)]
29. Nie, S.; Shen, W.; Shen, S.; Li, H.; Pan, Y.; Sun, Y.; Chen, Y.; Qi, H. Effects of Vacancy and Hydrogen on the Growth and Morphology of N-Type Phosphorus-Doped Diamond Surfaces. *Appl. Sci.* **2021**, *11*, 1896. [[CrossRef](#)]
30. Goss, J.P.; Briddon, P.R.; Jones, R.; Sque, S. Donor and acceptor states in diamond. *Diam. Relat. Mater.* **2004**, *13*, 684–690. [[CrossRef](#)]

31. Goss, J.P.; Briddon, P.R.; Eyre, R.J. Donor levels for selected n-type dopants in diamond: A computational study of the effect of supercell size. *Phys. Rev. B* **2006**, *74*, 2452171–2452177. [[CrossRef](#)]
32. Sque, S.J.; Jones, R.; Goss, J.P.; Briddon, P.R. Shallow donors in diamond: Chalcogens, pnictogens, and their hydrogen complexes. *Phys. Rev. Lett.* **2004**, *92*, 0174021–0174024. [[CrossRef](#)] [[PubMed](#)]
33. Yan, C.; Dai, Y.; Guo, M.; Huang, B.B.; Liu, D.H. Theoretical Characterization of Carrier Compensation In P-doped Diamond. *Appl. Surf. Sci. A J. Devoted Prop. Interfaces Relat. Synth. Behav. Mater.* **2009**, *255*, 3994–4000. [[CrossRef](#)]
34. Sakaguchi, I.; Mikka, N.; Kikuchi, Y.; Yasu, E.; Haneda, H.; Suzuki, T.; Ando, T. Sulfur: A donor dopant for n-type diamond semiconductors. *Phys. Rev. B* **1999**, *60*, R2139. [[CrossRef](#)]
35. Reiss, H. Chemical Effects Due to the Ionization of Impurities in Semiconductors. *J. Chem. Phys.* **1953**, *21*, 1209–1217. [[CrossRef](#)]

Disclaimer/Publisher’s Note: The statements, opinions and data contained in all publications are solely those of the individual author(s) and contributor(s) and not of MDPI and/or the editor(s). MDPI and/or the editor(s) disclaim responsibility for any injury to people or property resulting from any ideas, methods, instructions or products referred to in the content.